JOURNAL OF MATERIALS SCIENCE **36** (2001) 635–641

Mechanical and thermal induced chain conformational transformations in syndiotactic polypropylene (sPP)

M. BONNET, S. YAN, J. PETERMANN
Institute of Materials Science, Department of Chemical Engineering, University of Dortmund, D-44221 Dortmund, Germany
E-mail: petermann@chemietechnik.uni-dortmund.de

BIN ZHANG, DECAI YANG
Changchun Institute of Applied Chemistry, Chinese Academy of Sciences, 130022 Changchun, People's Republic of China

Stretching a stacked sPP lamellar morphology at room temperature leads to a mechanical induced transformation from the $(t_2g_2)_2$ (helical) into the (tttt) (zigzag) chain conformation of the polymer. The so prepared samples exhibit after annealing above 80°C a thermal induced retransformation into the cell I and cell III crystal structure of the helical chain conformation. The mechanical induced chain conformational transformation as well as the thermal induced retransformation was studied by means of transmission electron microscopy and electron diffraction.

1. Introduction

Since the first synthesis and characterization of stereoregular polypropylenes, i.e. isotactic and syndiotactic polypropylenes (iPP and sPP, respectively), by Natta *et al*. in the 1960s [1–4], the morphological studies of iPP were followed extensively [5–7], and sophisticated understanding on the molecular level has been achieved [8–11]. The sPP, due to the difficulties in its synthesis, has received much less attention, and the early work has not been continued for almost three decades. The development of the new metallocene catalyst systems made it possible to synthesize sPP with high stereoregularity [12]. As a result, the interest in the structural and morphological studies of sPP increased in the past few years.

SPP exhibits pronounced polymorphisms and morphologies, depending on its tacticity and thermomechanical treatments. Three different chain conformations in the crystalline state have been reported in the literature [13], i.e. (i) the helical $(t_2g_2)_2$ conformation formed from relaxed melts [14–16], (ii) the zigzag (tttt) chain conformation resulting from cold stretching [14, 17] or melt spinning of high tacticity chains (>95% pendent content) [18], and (iii) the $(t_6g_2t_2g_2)$ conformation produced by exposing the zigzag crystals to benzene, toluene or xylene vapor below 50°C [19]. Very recently, an additional chain conformation of (tg^+tg^-) was reported in highly oriented material [20]. The $(t_2g_2)_2$ conformation crystallizes in an orthorhombic system (cell I and cell III structure) [4, 21–23]. Many publications have already appeared on the mechanical and thermal induced chain conformational transformations for other polymers [24–32]. But detailed studies on mechanical and thermal induced chain conformational transformations for sPP are still missing.

The purpose of this paper is to present some experimental results regarding the mechanical and thermal induced chain conformational transformations of sPP.

2. Experimental

The materials used in this work are highly syndiotactic polypropylene (material A) with a stereoregularity of 97% pendant and a melting temperature of about 160°C, kindly supplied by Prof. Dr. Kaminsky from the University of Hamburg, Germany, and a second sPP (material B) with a stereoregularity of 85% pendant syndiotacticity, which is a pre-commercial product (EOD 96-30), kindly supplied by the FINA Oil & Chemical Company.

Highly oriented thin sPP films were prepared according to a melt-draw technique introduced by Petermann and Gohil [33]. The obtained films with a thickness of about 30–50 nm can be directly used for transmission electron microscopy (TEM) observations. Mechanical stretching of those melt-drawn films was performed with the help of soft (pre-polymerized) polyacrylic acid films having a thickness of about 2 mm. The polyacrylic acid films are still flexible at room temperature due to their low degree of polymerization. The oriented sPP films, supported by the polyacrylic acid, were stretched in a home made device. The stretching was performed in the orientation direction of the as-prepared sPP films. Subsequently, a thin carbon layer (ca 10 nm) was vacuum deposited onto the stretched film and the polyacrylic acid was dissolved in water. The stretched sPP films were finally mounted on TEM copper grids. For TEM observations, a Philips CM200 TEM operated at

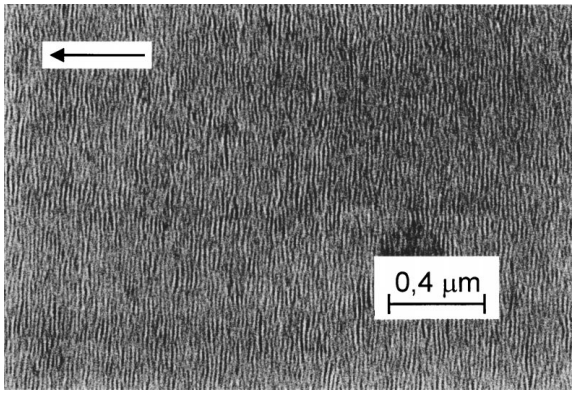

Figure 1 BF electron micrograph of a low tacticity sPP (materials B) melt-drawn film in the as drawn state. The arrow in the picture shows the drawing direction of the film.

200 kV was used in this study. Bright-field (BF) micrographs were obtained in the defocus imaging mode.

The thermal treatments were performed in a differential scanning calorimetry (DSC) 2910-system from TA Instruments in connection with a TA 2000 control system. Nitrogen was used for all treatments in order to avoid oxidation.

3. Results and discussion

3.1. Microstructure of sPP melt-drawn films in the as drawn state

Fig. 1 shows a BF electron micrograph of a melt-drawn sPP film (material B). The arrow in the picture indicates the drawing direction of the film. The gray lines in the micrograph reveal the crystalline lamellae of sPP

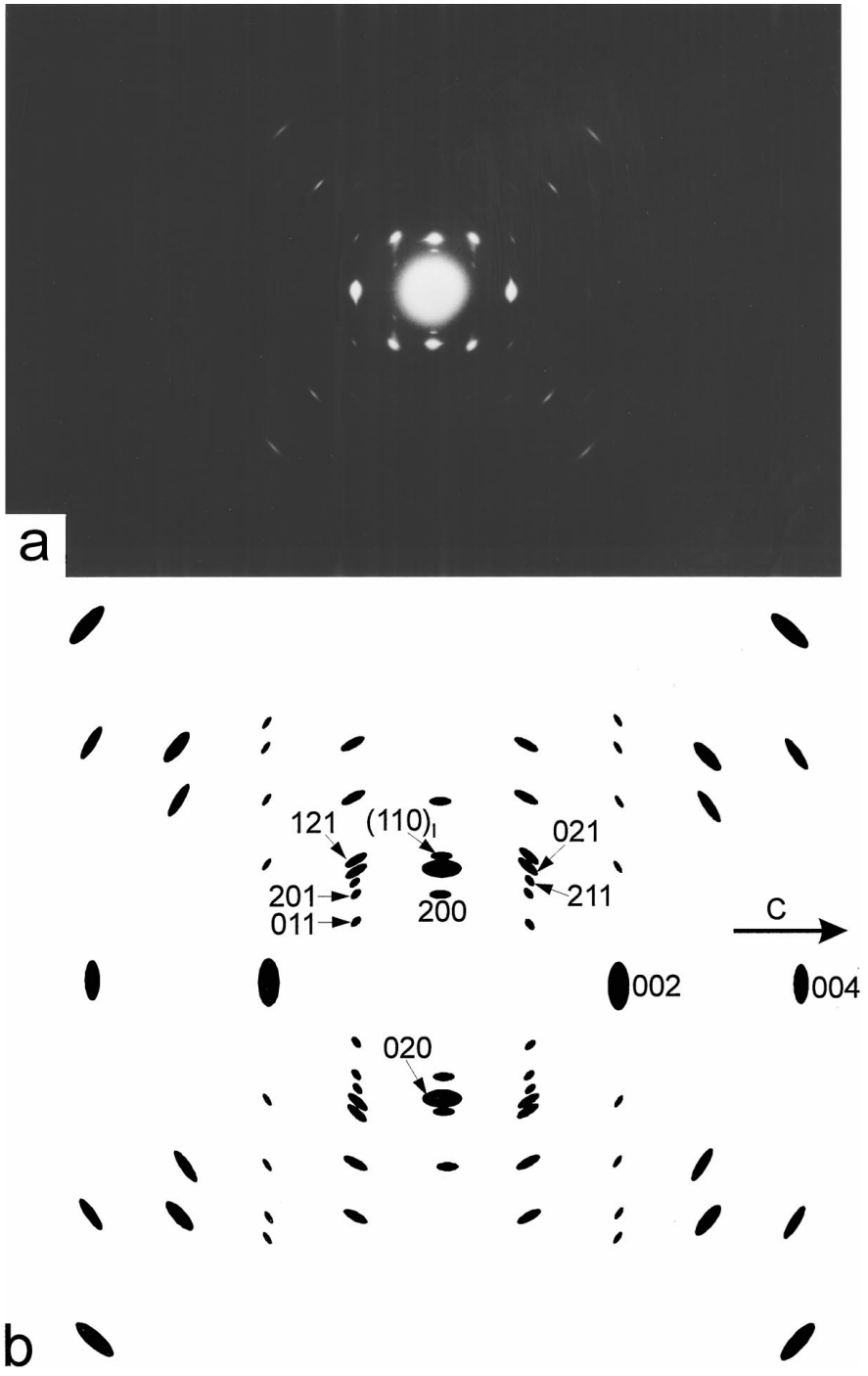

Figure 2 (a) Electron diffraction pattern and (b) its corresponding sketch with main reflections being indexed of the melt-drawn low tacticity sPP (material B) films.

(the dark parts of them are crystalline lamellae, which are oriented with respect to the electron beam such that Bragg orientational contrast occurs). The white regions, between the crystalline lamellae represent the amorphous areas. It can be seen that the sPP lamellae are well oriented perpendicular to the drawing direction. This implies a parallel alignment of the molecular chain direction of the sPP crystals in the drawing direction. The corresponding electron diffraction pattern and a sketch of it with main reflections indexed are shown in Fig. 2a and b. It reveals a typical electron diffraction pattern of the melt-drawn films and confirms the high orientation with the molecular chains in the film plane parallel to the drawing direction. The reflections can be indexed for the $(t_2g_2)_2$ sPP chain conformation with the unit cell III ($a = 1.45$, $b = 1.12$, and $c = 0.74$ nm) and cell I ($a = 1.45$, $b = 0.56$, and $c = 0.74$ nm) [4, 21]. Comparing the intensities of the reflection spots with those calculated from the structure factor of the cell III unit cell [21], in which the (200) reflection has the highest intensity, the intensity of the (200) reflection in the micrograph is much weaker than that of the (020) reflection, but the reverse intensities would be expected from the calculated structure factor. Our diffraction pattern can be explained by a double texture in which the *b*-axis of the sPP crystals is preferentially aligned in the film plane [18]. It should be pointed out, that additional reflection spots close to the (020) reflections can be identified. These reflection spots, as labeled in Fig. 2b with $(110)_I$, are indexed to the (110) for cell I.

The electron diffraction pattern of the high tacticity sPP (material A) melt-drawn films and a sketch of it with the main reflections indexed are shown in Fig. 3a and b. The drawing direction of the film is represented by an arrow. The diffraction pattern is clearly different from that shown in Fig. 2a. All the reflections in Fig. 3a can be indexed with the (tttt) chain conformation and the orthorhombic unit cell dimensions $a = 0.522$, $b = 1.117$, and $c = 0.506$ nm. From the intensities of the equatorial reflection spots, a fiber texture (and not a double texture as in the lower tacticity material) can be concluded [34]. Furthermore, streaks of the

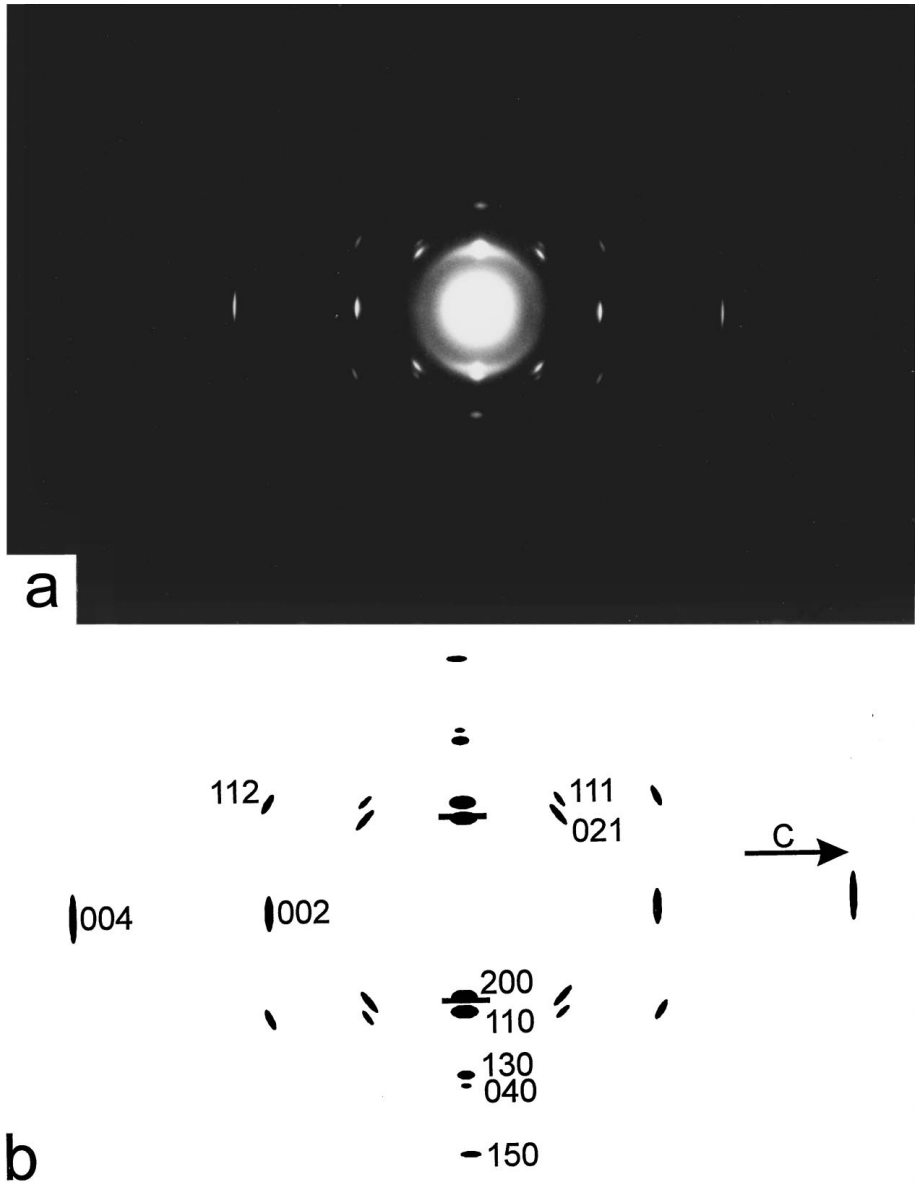

Figure 3 (a) Electron diffraction pattern and (b) its corresponding sketch with main reflections being indexed of the melt-drawn high tacticity sPP (material A) films.

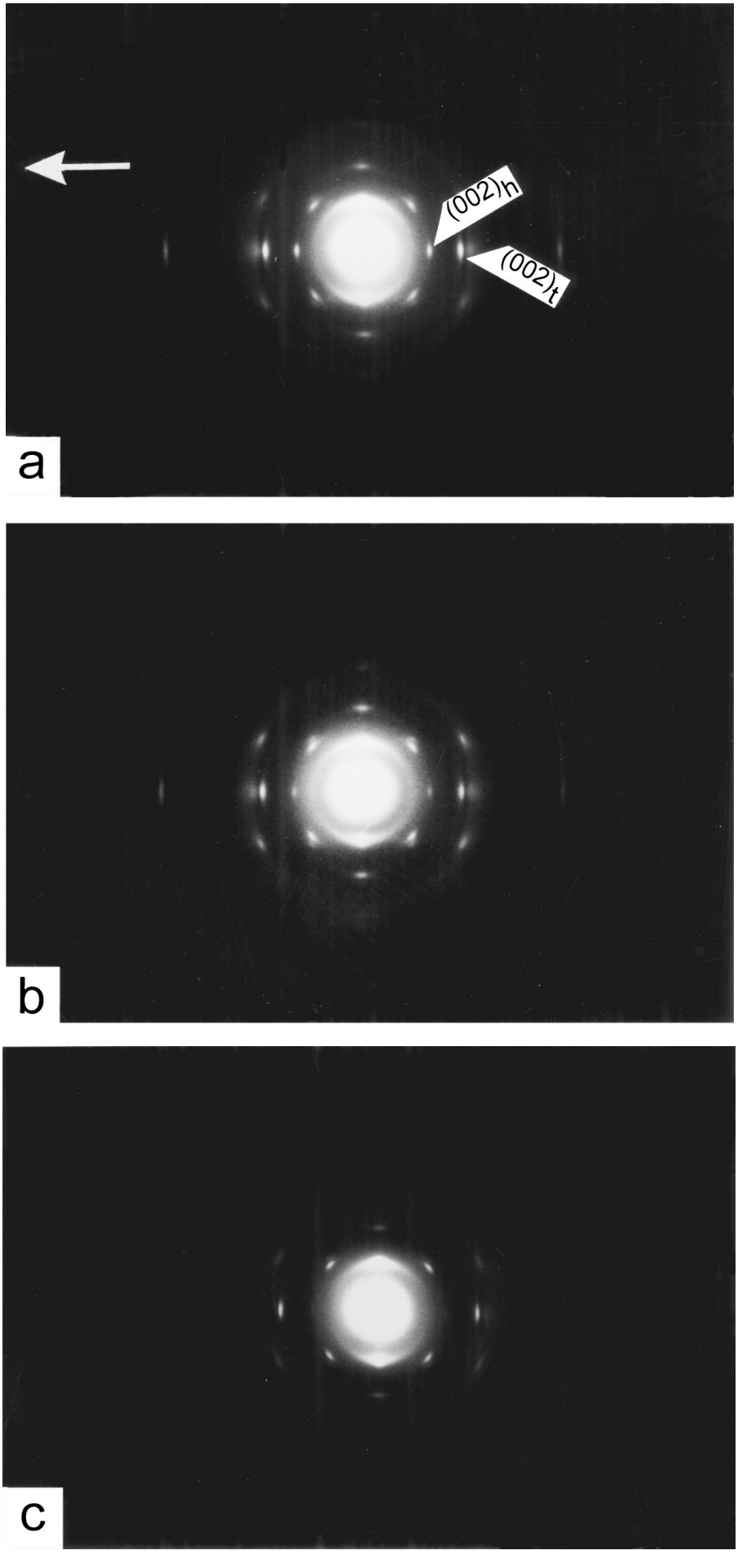

Figure 4 Electron diffraction patterns of melt-drawn low tacticity sPP (material B) films, which were subsequently deformed along its chain direction for (a) 50%, (b) 100%, and (c) 150%, respectively. The reflection spots associated to the helical and zigzag chain conformations are differentiated by the subscription “h” and “t”, respectively.

(200)-reflections in ⟨001⟩ direction are observed. These streaks may result from lattice defects in the (00*l*)-lattice-planes. The BF electron micrographs of these melt-drawn sPP (high tacticity) films with all-trans chain conformations do not exhibit a stacked lamellar structure. An oriented fringed micellar morphology is more likely, but this morphology is extremely difficult to image in the defocus contrast mode. Dark field electron micrographs, which should be able to image the micellar crystals, are also difficult to obtain due to the high radiation sensitivity of the polymer.

3.2. Mechanical induced chain conformational transformation

Fig. 4 shows the electron diffraction patterns of the melt-drawn sPP films (material B), which were further stretched in direction of their chain axis for (a) 50%, (b) 100%, and (c) 150%. The arrow indicates the stretching direction. While the $(002)_h$ reflection corresponds to the primary population of the crystallites with the $(t_2g_2)_2$ helix chain conformation, the $(002)_t$ is associated to the newly formed crystallites having the (tttt) zigzag chain conformation (Fig. 4a). This indicates, that by stretching parts of the sPP, helical crystals have transformed into zigzag chain crystals. The all-trans sPP crystal content increases with increasing the strain. When the oriented films are stretched 100% (Fig. 4b), the intensities of the $(002)_h$ reflections corresponding to the helical crystals are already weaker than those of the $(002)_t$ of the all-trans crystals. Stretching the melt-drawn films to 150%, the corresponding electron diffraction pattern (Fig. 4c) is identical to that shown in Fig. 3a and reflects a complete chain conformational transformation from helix to zigzag. Like in the melt-drawn high tacticity sPP (material B) (Fig. 3), streaks are also observed in all the diffraction patterns (Fig. 4a–c). They can be explained by an agglomaration of conformational defects in (00*l*) lattice planes and may result from a cooperative conformational transformation as speculated by Lotz *et al*. [35]. However, having a cooperative transformation process, a change of the double-textured initial films into double-textured transformed films would be more likely, but fiber textures are observed in the strain-transformed films (Fig. 4). The lamellar morphology in the as-prepared films vanishes after the mechanical induced transformation. No contrast is obtained in the TEM by the defocus imaging mode, probably for the same reason as in the as-prepared high syndiotactic films (micellar morphology).

3.3. Thermal induced chain conformational transformation

The electron diffraction pattern shown in Fig. 5 corresponds to samples (material B) which have been stretched to an extension of 150% and annealed at 120°C for 2 hrs. This diffraction pattern is similar to that shown in Fig. 2a. It reveals the $(t_2g_2)_2$ helical chain conformation and demonstrates a thermal induced retransformation from the zigzag to helix chain. But the relative intensities of the (*hk*0) and (*hk*1) reflections change significantly compared to those in Fig. 2a. This may result partly from the fact, that the sPP film now exhibits a fiber texture with the *c*-axis oriented still in the stretching direction but a random orientation of the *a*- and *b*-axes in the directions perpendicular to the *c*-axis. With the coexistence of the $(211)_{III}$ and $(110)_I$ reflections for cells III and I crystals in the diffraction pattern, respectively, the retransformation into both crystal structures is demonstrated. But additionally, a pronounced streaking of the (002) reflection is observed now and, moreover, intensity maxima in the streaks close to the (002) reflection spots are observed. These streaking intensity maxima can neither be related to the cell I nor the cell III crystal structure diffraction spots. They imply a periodical agglomeration of lattice defects in (*hk*0) planes, but the quality of the diffraction

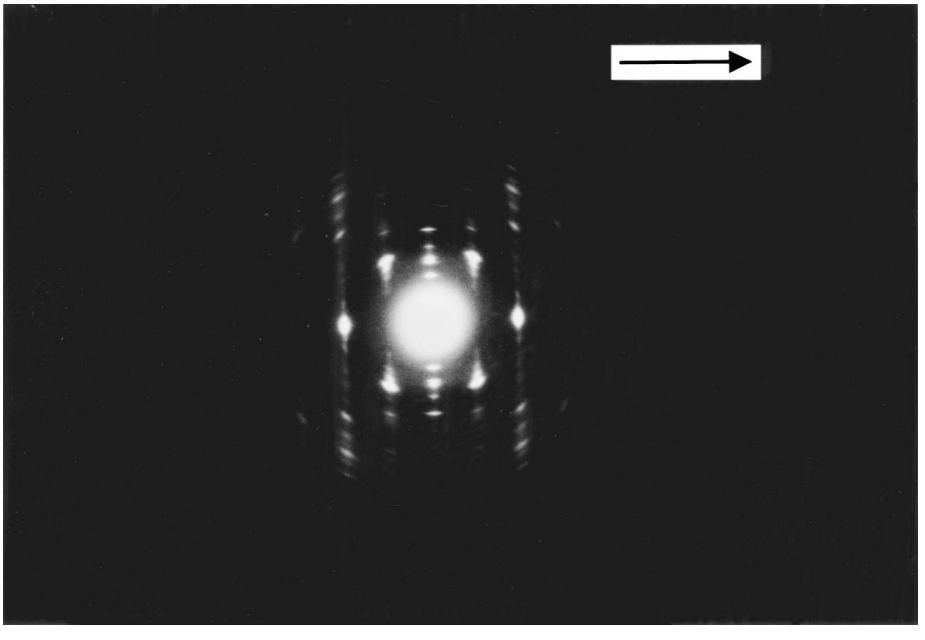

Figure 5 Electron diffraction pattern of a melt-drawn low tacticity sPP (material B) film, which was subsequently deformed along its chain direction for 150%, and then annealed at 120°C for 2 hrs. The arrow shows its chain direction.

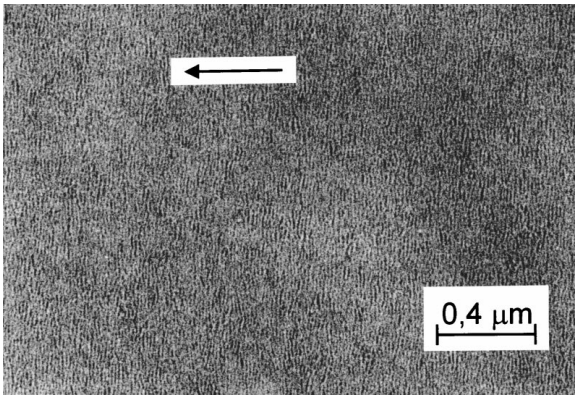

Figure 6 BF electron micrograph of a high tacticity sPP (materials A) melt-drawn film after thermal retransformation (120°C for 2 hrs). The arrow in the picture shows the drawing direction of the film.

photographs is not good enough to perform a more detailed analysis. From the intensity profiles of the diffraction spots it can clearly be seen that the crystal lattice obtained after the mechanical induced chain transformation (Fig. 4a–c) is much more disturbed than the crystal lattice after the thermal retransformation (Fig. 5).

After thermal retransformation, the micellar morphologies are changing into lamellar morphologies (Fig. 6). But in contrast to films from low tacticity sPP (material B), which retransforms from a fiber texture into a fiber texture, the high tacticity sPP (material A) retransforms from a fiber texture into a double texture (Fig. 7), which has the same lattice orientation as the as prepared material B (compare with Fig. 1).

While the streaking in the diffraction patterns are indicating that lattice defects (conformational defects, stacking faults etc.) are occurring after the conformational transformations, the loss and the appearance of double textures after the phase transformations and the morphological transformation from micellar into lamellar structures and vice versa (material B during mechanical induced transformation, material A after thermal induced transformation) are favoring a non cooperative molecular process (for example local melting and recrystallization) involved in the transformation.

4. Conclusion

The mechanical and thermal induced chain conformational transformations of sPP were studied by electron microscopy and electron diffraction. The results show that a chain conformation transformation from helix to zigzag can be achieved by high strains. To achieve complete transformation of a stacked lamellar structure, a strain of about 150% is necessary. A retransformation of the zigzag sPP chains into the helical chain conformation is achieved by thermal treatments above 80°C. A precise conclusion concerning the molecular process, which is involved in the transformation reaction, cannot be drawn from our results. But some observations give indications towards a non cooperative process.

Acknowledgment

The financial support of the Deutsche Forschungsgemeinschaft (DFG) and the Fonds der Chemischen Industrie (FCI) are gratefully acknowledged.

References

1. G. NATTA, I. PASQUON, P. CORRADINI, M. PERALDO, M. PEGORARO and A. ZAMBELLI, *Rend. Accad. Naz. Lincei* **28** (1960) 539.
2. G. NATTA, I. PASQUON and A. ZAMBELLI, *J. Amer. Chem. Soc.* **84** (1962) 1488.
3. A. ZAMBELLI, G. NATTA and I. PASQUON, *J. Polym. Sci. (C)* **4** (1963) 411.
4. P. CORRADINI, G. NATTA, P. GANIS and P. A. TEMUSSI, *ibid.* **16** (1967) 2477.
5. F. KHOURY, *J. Res. Natl. Bur. Std.* **70A** (1966) 29.
6. F. J. PADDEN and H. D. KEITH, *J. Appl. Phys.* **37** (1966) 4013.
7. *Idem., ibid.* **44** (1973) 1217.
8. A. J. LOVINGER, *J. Polym. Sci., Polym. Phys. Ed.* **21** (1983) 97.

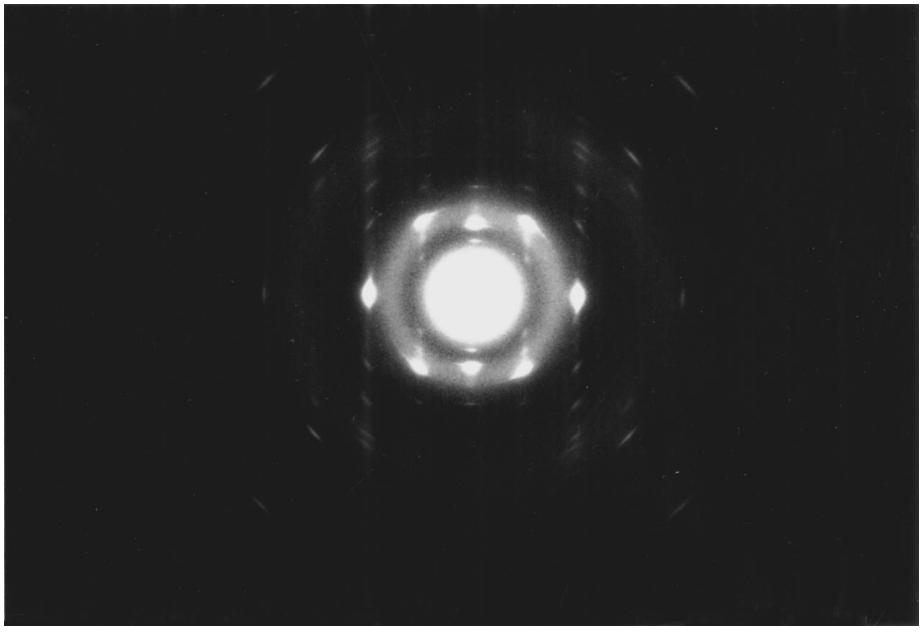

Figure 7 Electron diffraction pattern of the melt-drawn high tacticity sPP (material A) films after thermal transformation (120°C for 2 hrs).

9. B. LOTZ and J. C. WITTMANN, *ibid.* **24** (1986) 1541.
10. B. LOTZ, S. GRAFF and J. C. WITTMANN, *ibid.* **24** (1986) 2017.
11. S. BRÜCKNER and S. V. MEILLE, *Nature* **340** (1989) 455.
12. J. A. EVEN, R. J. JONES, A. RAZAVI and J. D. FERRARA, *J. Amer. Chem. Soc.* **110** (1988) 6255.
13. J. RODRIGUEZ-ARNOLD, Z. BU and S. Z. D. CHENG, *J. Macrom. Sci., Rev. C* **35** (1995) 117.
14. G. NATTA, M. PERALDO and G. ALLEGRA, *Makromol. Chem.* **75** (1964) 215.
15. G. NATTA, P. CORRADINI and P. GANIS, *ibid.* **39** (1960) 238.
16. *Idem., J. Polym. Sci.* **58** (1962) 1191.
17. J. LOOS, J. PETERMANN and A. WALDÖFNER, *Coll. Polym. Sci.* **275** (1997) 1058.
18. J. LOOS, A.-M. SCHAUWIENOLD, S. YAN, J. PETERMANN and W. KAMINSKY, *Polym. Bull.* **38** (1997) 185.
19. D. R. PAUL, *J. Polym. Sci.: Part B: Polym. Phys.* **29** (1991) 1649.
20. F. KATZENBERG, H. LIEBERTZ and J. PETERMANN, *Sen'i Gakkaishi* **53** (1997) 549.
21. B. LOTZ, A. J. LOVINGER and R. E. CAIS, *Macromolecules* **21** (1988) 2375.
22. A. J. LOVINGER, B. LOTZ and D. D. DAVIS, *Polymer* **31** (1990) 2253.
23. W. STOCKER, M. SCHUMACHER, S. GRAFF, J. LANG, J. C. WITTMANN, A. J. LOVINGER and B. LOTZ, *Macromolecules* **27** (1994) 6948.
24. R. JAKEWAYS, I. M. WARD, M. A. WILDING, I. J. DESBOROUGH and M. G. PASS, *J. Polym. Sci., Polym. Phys. Ed.* **13** (1975) 799.
25. I. M. WARD, M. A. WILDING and H. BRODY, *ibid.* **14** (1976) 263.
26. R. JAKEWAYS, T. SMITH, I. M. WARD and M. A. WILDING, *Polym. Lett. Ed.* **14** (1976) 41.
27. M. MILES and H. GLEITER, *J. Macromol. Sci.-Phys.* **B15** (1978) 613.
28. U. ALTER and R. BONART, *Colloid & Polym. Sci.* **258** (1980) 332.
29. P. L. TAYLOR, *Mat. Sci. Forum* **4** (1985) 105.
30. K. W. CHAU, Y. C. YANG and P. H. GEIL, *J. Mater. Sci.* **21** (1986) 3002.
31. K. NAKAMURA, T. AOIKE, K. USAKA and T. KANAMOTO, *Macromolecules* **32** (1999) 4975.
32. R. M. GOHIL, M. J. MILES and J. PETERMANN, *Macromol. Sci.-Phys. B* **21** (1982) 189.
33. J. PETERMANN and R. M. GOHIL, *J. Mater. Sci. Lett.* **14** (1979) 2260.
34. Y. CHATANI, H. MARUYAMA, K. NOGUCHI, T. ASANUMA and T. SHIOMURA, *J. Polym. Sci.: Part C: Polym. Lett.* **28** (1990) 393.
35. B. LOTZ, C. MATHIEU, A. THIERRY, A. J. LOVINGER, C. DE ROSA, O. RUIZ DE BALLESTEROS and F. AURIEMMA, *Macromolecules* **31** (1998) 9253.

Received 23 September
and accepted 19 October 1999